Adiabatic frequency conversion of optical information in atomic vapor

Frank Vewinger,[1,2] Jürgen Appel,[1] Eden Figueroa,[1] and A. I. Lvovsky[1,*]

[1]*University of Calgary, Calgary, Alberta T2N 1N4, Canada*
[2]*Present address, Institut für Angewandte Physik, Universität Bonn, Wegelerstr. 8, 53115 Bonn, Germany*
[*]*Corresponding author: lvov@ucalgary.ca*

Received June 1, 2007; revised July 30, 2007; accepted August 12, 2007;
posted August 14, 2007 (Doc. ID 83486); published September 17, 2007

We experimentally demonstrate a communication protocol that enables frequency conversion and routing of quantum information in an adiabatic and thus robust way. The protocol is based on electromagnetically induced transparency (EIT) in systems with multiple excited levels: transfer and/or distribution of optical states between different signal modes is implemented by adiabatically changing the control fields. The proof-of-principle experiment is performed using the hyperfine levels of the rubidium $D1$ line. © 2007 Optical Society of America

OCIS codes: 270.5530, 020.1670, 190.4380, 300.6210, 190.2620.

An essential element of a quantum optical communication network is a tool for transferring and/or distributing quantum information between optical modes (possibly of different frequencies) in a loss- and decoherence-free fashion [1]. This is important not only for routing quantum information, but also for interfacing quantum communication lines of different wavelengths (e.g., fiber-optical and open-air) between each other and with memory-based quantum repeaters [2,3]. Some experiments on frequency conversion of quantum states of light have been performed using nonlinear optical effects in crystals [4–6] and periodically poled waveguides [7]. An alternative approach [8,9] involves storage of light by means of electromagnetically induced transparency (EIT) [10] and its subsequent retrieval on another optical transition.

In this Letter, following our group's recent proposal [11], we experimentally demonstrate a protocol for routing and frequency conversion of optical quantum information via EIT in an atomic system with multiple excited levels. Our method is related to that of [8,9], but here the information is transferred *during the propagation*, thus avoiding the necessity of storage. By means of the EIT control fields we steer the composition of the optical component of the dark-state polariton (DSP) and can convert, completely or partially, the incoming signal state into another optical mode. Our scheme (which we call RATOS, Raman adiabatic transfer of optical states) resembles stimulated Raman adiabatic passage (STIRAP) [10], but applies to optical rather than atomic states. Thanks to its adiabatic character, the efficiency of RATOS does not strongly depend on the parameters of the control fields, but only on their initial and final values, which is favorable for possible practical applications of the method.

We consider a double-Λ system implemented by the rubidium-87 $D1$ transition, where the ground $5S_{1/2}$ and excited $5P_{1/2}$ levels are each split into two hyperfine sublevels as shown in Fig. 1(a). For simplification, we neglect the degenerate Zeeman substructure and thus the existence of competing dark states [12]. The energy levels are coupled by two weak signal fields, described by their annihilation operators $\hat{a}_1$ and $\hat{a}_2$, and two strong control fields, described by their Rabi frequencies Ω_1 and Ω_2. Such a system exhibits EIT for the superposition

$$\hat{b} \propto \left[\frac{\Omega_1}{g_1}\hat{a}_1 + \frac{\Omega_2}{g_2}\hat{a}_2 \right] \tag{1}$$

of the signal fields, with g_i being the vacuum Rabi frequency for the ith signal mode [11,13,14,16].

RATOS proceeds as follows: with only control field Ω_1 (hereafter called pump) initially present, a pulsed optical state in mode $\hat{a}_1$ (signal) is coupled into the medium. While it is propagating, control field Ω_2 (retrieve) is turned on slowly, so the EIT signal mode is adiabatically converted into superposition (1), which continues to propagate losslessly through the cell [11]. If the pump field is left on, the optical state that has entered the cell in mode $\hat{a}_1$ will leave it in mode $\hat{b}$. This allows the implementation of beam splitting for optical modes of different frequency, with the final intensities of the two control pulses determining the outcome of the process. The beam splitting ratio is given by

$$\frac{\langle \hat{a}_2 \rangle}{\langle \hat{a}_1 \rangle} = \frac{g_1 \Omega_2}{g_2 \Omega_1}. \tag{2}$$

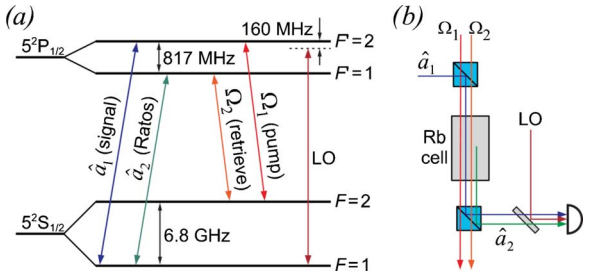

Fig. 1. (Color online) (a) Transitions used in the experiment, as described in the text. Also shown is the local oscillator field (LO) used for heterodyne detection. (b) Sketch of the experimental setup. In the actual experiment, the beams are overlapping in the cell; the separation in the drawing is for clarity.

0146-9592/07/192771-3/$15.00

If the pump field is instead adiabatically switched off while mode $\hat{b}$ is still inside the cell, the initial quantum state of mode $\hat{a}_1$ will be transferred to the Ratos mode $\hat{a}_2$, thus completing the RATOS protocol [11].

The experiment was performed in warm rubidium-87 vapor at 60°C in a 5 cm long cell filled with 10 Torr of neon as a buffer gas. The cell was mounted within a magnetically shielded oven. The signal field was provided by a Coherent MBR-110 Ti:sapphire laser. The pump and retrieve fields were obtained from external-cavity diode lasers sequentially phase locked to each other and the Ti:sapphire laser. The frequency difference among the three fields entering the cell corresponded to the hyperfine splitting frequencies of the ground and excited levels of the rubidium $D1$ transition: 6835 and 817 MHz, respectively. All three laser beams were controlled by acousto-optical modulators. All polarizations were linear, with the polarization of the control beams orthogonal to that of the signal and Ratos beams.

After passing through the cell, the two signal fields were separated from the control beams using a polarizing beam splitter, and subjected to heterodyne detection on a fast photodiode [Fig. 1(b)]. The role of the local oscillator was played by the unmodulated Ti:sapphire laser. The beat note at 160 MHz (signal field) or 657 MHz (Ratos field) was measured by using a spectrum analyzer in the zero span mode, with a temporal resolution of 200 ns.

We performed a set of preliminary measurements to verify the functionality of our setup. First, with all three input fields continuously on, we observed generation of a field on the Ratos transition due to four-wave mixing. Second, we checked that the signal field experienced EIT when only the pump was present and observed slowdown of the 400 ns signal pulse. Third, we performed a classic storage of light experiment [3] by turning the pump field off after the signal pulse entered the cell and turning it back on after a few hundred microseconds. Fourth, we stored the signal pulse and then recovered it on the Ratos transition by using the retrieve field akin to Zibrov and coworkers [8]. Finally, by reducing the delay Δt between the turn-off of the pump and the turn-on of the retrieve field to small negative values, we observed RATOS.

Figure 2 shows the retrieved pulse waveforms with the delay varied between −0.5 and 2 μs. In contrast to optical storage ($\Delta t > 0$), the position of the retrieved pulse in the RATOS regime ($\Delta t < 0$) does not strongly depend on Δt. This is because in the absence of storage, the timing of the Ratos pulse is determined solely by the propagation of the DSP through the cell. On the other hand, there is clear difference between RATOS and classic four-wave mixing. In the latter, the electric field of the created mode is proportional to that of the three mixing fields: $\langle \hat{a}_2 \rangle \propto \Omega_1 \Omega_2 \langle \hat{a}_1 \rangle$. In contrast, the RATOS pulse is produced when two of these fields are no longer present.

If the retrieve field is present *before* the signal pulse enters the cell, the initial EIT mode (1) is not equal to $\hat{a}_1$ and the signal is partially absorbed,

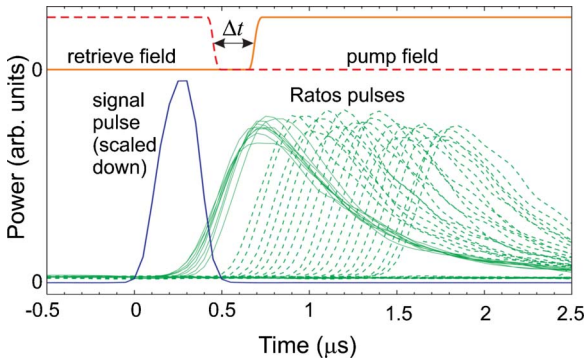

Fig. 2. (Color online) Temporal profiles of the fields. Ratos pulses are shown for the case in which the retrieve field is turned on before (solid curves) and after (dashed curves) the pump field has been turned off. The pump, retrieve, and signal field powers were, respectively, 8300, 7400, and 0.4 μW.

which in theory would compromise the RATOS efficiency. However, in our experimental conditions this loss was not pronounced due to a competing effect: the added retrieve field increased the visibility of the EIT line on the signal transition.

We further verified the adiabatic nature of RATOS by varying the intensity of the retrieve field and monitoring the shape of the output Ratos pulse. As expected (Fig. 3), the time-integrated intensity of the Ratos pulse shows only a weak dependence of the created field mode for sufficiently high retrieve field intensities. With the retrieve field below 2 mW, the EIT effect was not sufficiently pronounced; so the Ratos pulse experienced partial absorption. The residual dependence for higher powers is due to a Gaussian geometric profile of the control fields resulting in poor EIT in the wings of the beams.

The Ratos pulse *shape*, on the other hand, depends strongly on the control field parameters. As evidenced by Fig. 3, the peak intensity and the temporal width of the Ratos pulse are, respectively, proportional and inversely proportional to the power of the retrieve laser Ω_2. The width of the Ratos pulse is inversely proportional to the spectral width of the EIT resonance [17], which, in a Doppler-broadened,

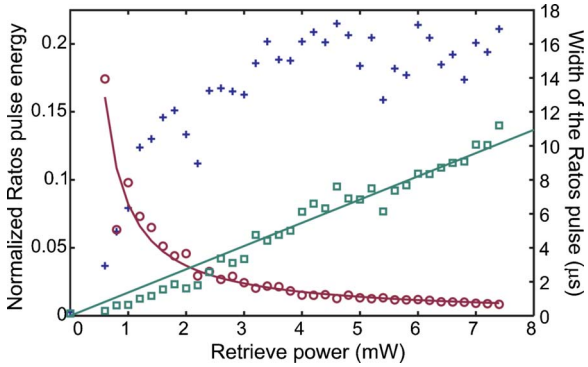

Fig. 3. (Color online) Peak power of the retrieved Ratos pulse (□), its temporal width (○), and energy (+) as a function of the power of the retrieve laser for a pump power of 4 mW. The energy is normalized to the energy of the slowed down pulse. The peak intensity plot is in arbitrary units. The solid lines are linear and inverse linear fits.

weakly decohering medium is essentially proportional to the control field intensity [18].

To realize an optically controlled beam splitter, the pump field Ω_1 was kept on continuously at 4 mW, while Ω_2 was turned on after the signal pulse had fully entered the rubidium cell. In this case the quantum state of the signal mode $\hat{a}_1$ was transferred into a superposition $\hat{b}$ of the modes $\hat{a}_i$, given by Eq. (1). The three waveforms of the output signal and Ratos fields at different retrieve field powers [Fig. 4(a)] illustrate the dynamics of multimode DSPs in the EIT medium. Even though the pump field remains the same in all three plots, the group velocity of the signal pulse (which couples to the pump field through an excited level) increases with the retrieve field intensity. This happens because in the presence of the retrieve field, the signal is no longer an independent EIT mode, but a part of a multimode DSP whose group velocity is proportional to the weighted quadratic mean of all the control Rabi frequencies [11].

Figure 4(b) displays the energy ratio of the Ratos and output signal fields as a function of the retrieve intensity. The observed proportional dependence is explained by Eqs. (1) and (2): the fraction of a particular signal field in a multimode polariton is proportional to the Rabi frequency of the associated control field. The observed deviation from the linear fit is due to a systematic error in evaluating the output signal energy: at high retrieve powers, the signal is small; so the relative error increases.

If the energy of the retrieved pulse is plotted against the power of the retrieve field, a dependence given by $P_{\mathrm{Ratos}}=P_{\mathrm{signal}}P_{\mathrm{ret}}/(CP_{\mathrm{pump}}+P_{\mathrm{ret}})$ can be derived from Eq. (1), where C is a constant depending on the oscillator strengths and the beam radii. In Fig. 4(c), this function is fitted to the data, with an overall coefficient included to account for the efficiency of the process. The fit yields a transfer efficiency of 70% with respect to the slowed down pulse, or up to 42% relative to the incoming signal pulse.

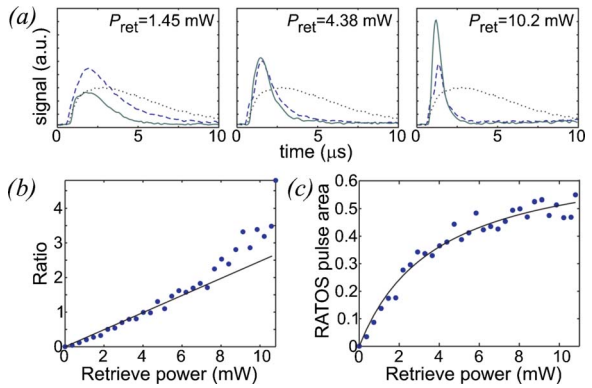

Fig. 4. (Color online) Beam splitting via RATOS. (a) Example waveforms for different retrieve pulse powers P_{ret} and P_{pump}=4 mW. The Ratos field ($\hat{a}_2$) is shown with a solid curve, the transmitted signal ($\hat{a}_1$) with a dashed curve. The dotted curve displays the transmitted, slowed down signal pulse in the absence of the retrieve field (regular EIT). (b) Energy ratio of the Ratos pulse and the transmitted signal pulse, as a function of the retrieve field power. (c) Energy of the restored Ratos pulse normalized to the energy of the slowed down pulse [dotted curve in Fig. 4(a)]; the solid curve is a theoretical fit.

In summary, we have demonstrated the possibility for adiabatic frequency conversion and routing of optical information carried by light between two signal modes in a multi-Λ EIT configuration. We foresee that RATOS will be useful in a variety of quantum commumnication and quantum engineering applications. Of special interest is the extension of RATOS to solid state-systems [19], where the level structure allows access to nearly arbitrary frequencies.

The measurements have been performed using classical light pulses; thus the efficient transfer of the quantum state is yet to be demonstrated. To this end we have set up a narrowband parametric quantum light source [20], which can be used to verify conservation of a quantum state during the transfer.

This work was supported by NSERC, CIAR, AIF, CFI, and Quantum *Works*. We appreciate helpful discussions with K.-P. Marzlin.

References

1. http://www.iqis.org/.
2. L. M. Duan, M. Lukin, J. I. Cirac, and P. Zoller, Nature **414**, 413 (2001).
3. D. F. Phillips, A. Fleischhauer, A. Mair, R. L. Walsworth, and M. D. Lukin, Phys. Rev. Lett. **86**, 783 (2001).
4. S. Tanzilli, W. Tittel, M. Halder, O. Alibart, P. Baldi, N. Gisin, and H. Zbinden, Nature **437**, 116 (2005).
5. J. Huang and P. Kumar, Phys. Rev. Lett. **68**, 2153 (1992).
6. G. Giorgi, P. Mataloni, and F. D. Martini, Phys. Rev. Lett. **90**, 027902 (2003).
7. A. P. Vandevender and P. G. Kwiat, J. Mod. Opt. **51**, 1433 (2004).
8. A. S. Zibrov, A. B. Matsko, O. Kocharovskaya, Y. V. Rostovtsev, G. R. Welch, and M. O. Scully, Phys. Rev. Lett. **88**, 103601 (2002).
9. B. Wang, S. Li, H. Wu, H. Chang, H. Wang, and M. Xiao, Phys. Rev. A **72**, 043801 (2005).
10. M. Fleischhauer, A. Imamoglu, and J. P. Marangos, Rev. Mod. Phys. **77**, 633 (2005).
11. J. Appel, K.-P. Marzlin, and A. I. Lvovsky, Phys. Rev. A **73**, 013804 (2006).
12. R. G. Unanyan, B. W. Shore, and K. Bergmann, Phys. Rev. A **59**, 2910 (1999).
13. X.-J. Liu, H. Jing, and M.-L. Ge, Eur. Phys. J. D **40**, 297 (2006).
14. S. A. Moiseev and B. S. Ham, Phys. Rev. A **73**, 033812 (2006).
15. E. Cerboneschi and E. Arimondo, Phys. Rev. A **52**, R1823 (1995).
16. E. Cerboneschi and E. Arimondo, Phys. Rev. A **54**, 5400 (1996).
17. M. D. Lukin and A. Imamoğlu, Phys. Rev. A **84**, 1419 (2000).
18. E. Figueroa, F. Vewinger, J. Appel, and A. I. Lvovsky, Opt. Lett. **31**, 2625 (2006).
19. A. V. Turukhin, V. S. Sudarshanam, M. S. Shahriar, J. A. Musser, B. S. Ham, and P. R. Hemmer, Phys. Rev. Lett. **88**, 023602 (2002).
20. J. Appel, D. Hoffman, E. Figueroa, and A. I. Lvovsky, Phys. Rev. A **75**, 035802 (2007).